

Latency Modeling of Hyperledger Fabric for Blockchain-based IoT (BC-IoT) Networks

Sungho Lee, Minsu Kim, Jemin Lee, *Member, IEEE*,
Ruei-Hau Hsu, *Member, IEEE*, and Tony Q. S. Quek, *Fellow, IEEE*

Abstract—With the worldwide growth of IoT industry, the need for a strong security level for IoT networks has also increased, leading to blockchain-based IoT (BC-IoT) networks. While blockchain technology is leveraged to ensure data integrity in a distributed manner, Hyperledger Fabric (HLF) attracts attention with its distinctive strong point without requiring the power-consuming consensus protocol, that is, proof-of-work (PoW). However, even though such security concerns can be mitigated using HLF, the additional processing time spent in HLF may emerge as another issue because most IoT devices handle real-time and latency critical jobs. This problem still remains unresolved because of the absence of a HLF latency model and a parameter setup guideline to reducing the mean latency. In this paper, therefore, we develop a HLF latency model for HLF-based IoT networks based on probability distribution fitting, by which mean latency prediction is facilitated once probable configuration environments are determined, in terms of the block size, block-generation timeout, and transaction generation rate parameters. Furthermore, we conclude by analyzing the impacts of influential HLF parameters on the mean latency, in order to provide insights not only on optimizing the mean latency, but also on coping with long mean latency.

I. INTRODUCTION

Blockchain technology has been widely studied since the first paper on Bitcoin was published to propose a new type of electronic monetary system. The paper points out the single point of failure (SPOF) problem stemming from the current centralized cash system with a central authority, and provides a solution building a distributed monetary system to the SPOF problem. Based on the underlying structure of the solution, which is blockchain, a whole variety of blockchain-based distributed platforms have emerged with different purposes from one another, accompanying a wide range of blockchain-related applications and research topics. As one of the examples, a blockchain-based IoT (BC-IoT) network is introduced to fulfill new security requirements of IoT environments. Considering blockchain technology can not only ensure data integrity, but also ameliorate security concerns in a distributed manner, various blockchain platforms have been explored and discussed for IoT devices with limited resources [1].

Corresponding author is J. Lee.

S. Lee, M. Kim, and J. Lee are with Daegu Gyeongbuk Institute of Science and Technology (DGIST), 333, Techno Jungang-daero, Daegu, Republic of Korea 42988 (e-mail: {seuho2003, kms0603, jmnlee}@dgist.ac.kr).

R.-H. Hsu is with National Sun Yat-sen University, 70 Lienhai Rd., Kaohsiung 80424, Taiwan, R.O.C. (e-mail: rhhhsu@mail.cse.nsysu.edu.tw).

T. Q. S. Quek is with Information Systems Technology and Design Pillar, Singapore University of Technology and Design, Singapore 487372 (e-mail: tonyquek@sutd.edu.sg).

The BC-IoT network refers to a particular IoT network whose underlying structure is on the basis of blockchain technology for IoT device data management. For a blockchain system, it is imperative to select a consensus protocol for data integrity. Although proof-of-work (PoW) is the most popular and general choice, it is too power-consuming to be unsuitable for power-constrained IoT devices because it is mandatory for miners to continually solve hash puzzles for data integrity. In this sense, Hyperledger Fabric (HLF) deserves consideration as HLF-based IoT networks because it supports a couple of alternative consensus methods without burdening IoT devices with high power consumption. Besides, its strict membership rule not only prevents privacy leakage, but also enables excluding unauthorized access, prohibiting attackers from working as legitimate members in HLF-based IoT networks.

However, from the viewpoint of IoT devices that handle real-time jobs, it is also important to take the HLF latency into account on top of security concerns. Otherwise, they may fail to accomplish latency critical tasks on time. In this sense, it is desirable to predict and reduce the mean latency in order to prevent time sensitive jobs from spending too long time in HLF. However, the absence of a HLF latency model leaves this problem unsettled. To be specific, HLF has a sophisticated structure, in which several different nodes and components simultaneously affect the performance, which will be explained in detail in Section III. It signifies that there exist many considerations for the optimal parameter setup to achieve the lowest latency. In addition, the structural complexity causes difficulty in constructing a testbed blockchain network, complicating performance evaluation of every use case and scenario. Thus, it is almost impossible to fulfill the lowest latency without a HLF latency model.

In this paper, we establish a latency model of HLF for a specific BC-IoT network (i.e., a HLF-based IoT network), in which latency critical tasks are generally handled. We also focus on two important blockchain parameters (i.e., block size and block-generation timeout), and analyze their impacts on the mean latency to provide guidelines to reducing it. The contributions of this paper are listed in detail as follows:

- We leverage HLF v1.3 other than obsolete one (i.e., HLF v0.6) for latency modeling. Providing a latency model based on probability distribution fitting, we exhibit that the total latency of HLF is modeled with the gamma distribution within a certain configuration range. This contributes not only to forecasting the mean latency of HLF-based IoT networks in practice, but also to preparing

the optimal setup for the lowest latency.

- Focusing on the block size and block-generation timeout, we analyze their impacts on the mean latency with varying their configuration values. This analysis contributes to comprehending the methods for decreasing the mean latency from each parameter's perspective.

The remainder of this paper is organized as follows: Section II discusses related work and limitations. Section III provides a brief overview of HLF based on the internal transaction flow and essential components, instantiating HLF-based IoT networks. Section IV explains the methodology for probability distribution fitting and proposes our latency model. Section V discusses the impacts of two influential HLF parameters on the mean ledger-commitment latency. Lastly, the conclusions of this paper are organized in Section VI.

II. RELATED WORK

In this section, we introduce previous work that evaluates the performance of HLF in various aspects (e.g., throughput, latency, scalability, etc.), and that provides a performance model. Especially, the former studies are usually focused on assessing and exploring performance trends with various HLF setups as well as in different environments from each other [2]–[8].

Some studies are based on the obsolete version, which is HLF v0.6. The performance of HLF v0.6 is compared to that of other private blockchain platforms (i.e., Ethereum and Parity) in [2] and [3]. These papers explore their performance differences among the three private blockchain platforms, using a newly developed framework that they propose to benchmark private blockchains. Another comparative study between Ethereum and HLF v0.6 is conducted in [4]. In [4], their performance differences in the execution time, average latency, and throughput are explored with varying number of transactions, especially when the blockchain networks are congested due to many transactions.

Since HLF v1.0, it has a different structure from the obsolete version. Therefore, many researchers lately focus on the new version when evaluating the performance of HLF. An empirical study is conducted to understand the overall performance of HLF with varying blockchain parameter values [5]. In [5], experiments are performed to reveal how HLF performance trends are changed with controllable parameters. Besides, simple optimizations for improving the overall system performance are also performed based on the action items that they list. With emphasis on the block size and batch-timeout (i.e., block-generation timeout), the effects of the two parameters on the average throughput and latency are empirically demonstrated in [6]. In particular, this paper considers that an increase in number of endorsing peers may also affect the performance. Another performance evaluation study is conducted in [7]. This paper considers three parameters and perform experiments for each case to evaluate HLF against three performance metrics: throughput, latency, and scalability. Note that specific parameters considered in [7] are transaction arrival rates, number of transactions, and number of simultaneous transactions. The performance differences between

the old version and the new version of HLF are explored in [8]. Specifically, with the various number of total generated transactions, this paper mainly shows how an invoke function and query function affect the execution time, average latency, and throughput in the different two versions of HLF.

Particularly, some studies explore the performance from the perspective of specific cases in [9] and [10]. As one of the specific use case studies, a HLF network dedicated to IoT applications is discussed to evaluate and improve its performance [9]. In [9], a new algorithm using multi-batched scheduling method, which is called as *Accelerator*, is proposed and leveraged to assess the established HLF network for IoT devices against two performance metrics: throughput and latency. Data updates in HLF occurs in all organizations, where the data are retained, and the next block to update the ledger has to await until the previous one is completely committed in all the participating organizations. In this sense, the impact on the performance is observed when block propagation is intentionally impeded in [10].

The HLF components-related performance is evaluated in [11]–[13]. HLF supports several different programming languages to construct a chaincode, which is also referred to as a smart contract. In [11], performance differences among the available languages are explored for a query and invoke request. Practical Byzantine fault tolerance (PBFT) is to enable a distributed system to endure malicious behavior and node failures. This protocol is provided as a consensus protocol in HLF v0.6. In [12], performance evaluation of a PBFT-based ordering service is performed with designing malicious behavior cases, and this shows that malicious behavior is also impactful upon the performance. Every peer in HLF possesses a database to store data. During the data update process, each transaction in a block updates the database. With regard to this process, the database system performance is characterized in [13]. In addition, performance improvement is fulfilled by GoLevelDB optimization work. However, even though the aforementioned research [2]–[13] helps to understand the comprehensive performance trends of HLF, it cannot be used to predict the performance of a HLF network with a given parameter setup.

System modeling studies have been performed to design performance models of HLF [14]–[17]. The PBFT consensus process, which is the consensus protocol in HLF v0.6, is modeled with empirically obtained data using stochastic reward nets (SRNs) in [14]. Based on the proposed SRN model, the scalability of PBFT is estimated by measuring the mean time to finish the consensus process with large number of nodes. In [15], furthermore, for the entire transaction-processing stages of HLF, a performance model of HLF with a Kafka/ZooKeeper-based ordering service is designed using SRNs. The proposed SRN model of HLF is on the basis of test runs, which are performed to decide appropriate parameter values inside the SRN model. An analytical model of a HLF-based system is proposed in [16] using generalized stochastic petri nets (GSPN). Furthermore, this paper also identifies the performance bottleneck based on the GSPN model and proposes a mathematical configuration selection approach to achieve the best throughput. In order to analyze the transaction

process performance of HLF, a hierarchical model of HLF is developed in [17]. The model accuracy is assessed through numerical analysis and simulations. The aforementioned HLF modeling studies have at least one of the limitations in the following: PBFT does not currently available since HLF v1.0, but works with the obsolete version only (i.e., HLF v0.6). Although a minor version of HLF v1.3 tailored for PBFT has been implemented, it is not an official release [18]. Therefore, it is difficult to consider that performance models of HLF v0.6 with PBFT are practical for now. Besides, the distributions of HLF latency types have not been explored until the present, leading to difficulty in analyzing the HLF system in a stochastic manner.

III. HYPERLEDGER FABRIC OVERVIEW

The Hyperledger Project aims to promote blockchain technology by fostering open-source blockchain frameworks, various blockchain tools, and blockchain libraries [19]. In contrast to the previous blockchain platforms, where deterministic programming languages are compulsory to prohibit ledgers from diverging, HLF, which is one of the frameworks of this project, is to develop a private modular blockchain platform not only enabling several business logics to be written in general-purpose programming languages, but also preventing blockchain forks [20]. In order to support non-deterministic programming languages and to avoid blockchain forks simultaneously, HLF adopts a novel structure, in which transactions go through three phases. In this section, we first provide the definitions of some significant system components and parameters in HLF, then demonstrate the three-phased transaction flow. Note that we refer to the Hyperledger official website and Read the Docs [19] [21] to define the system components with accuracy in this paper.

A. System Components

1) *Peer*: The peer refers to a node which serves as a member in a HLF network. In HLF, the peer is mainly classified under three types: committing peer (i.e., committer), endorsing peer (i.e., endorser), and ordering peer (i.e., orderer).

- The committing peer refers to a normal peer allowed to maintain a copied ledger and to validate newly delivered blocks. Note that committing peers are not empowered to play the unique roles of endorsing and ordering peers (e.g., transaction proposal simulation, transaction ordering, and block generation).
- The endorsing peer refers to a particular committing peer entitled to hold and to access smart contracts, with which transaction proposals from clients are simulated against their copied ledgers. In other words, endorsing peers are referred to as particular peers qualified for generating each of their simulation results of transaction proposals based on the copied ledgers, using smart contracts.
- The ordering peer refers to a node consisting of the ordering service that is a node cluster taking charge of arranging transactions in chronological order and producing a new block. Ordering peers perform the pre-defined consensus protocol on the new block, then the block is conveyed to peers via the gossip protocol.

2) *Channel*: The channel is a sub-network, in which a set of peers are gathered together for data confidentiality. Every channel is registered by the ordering service in the channel configuration block generated by the blockchain service provider, therefore, a peer is required to submit the channel configuration block when joining a channel as a new member. The peers in the same channel may belong to different organizations from one another, however, they share and maintain the identical ledger without allowing the other peers to tamper the ledger. In this paper, we call this channel component as a HLF channel in order to avoid confusion.

3) *Ledger*: The ledger is composed of a blockchain and the state database. The blockchain includes all transactions, which have been generated until the present as a immutable chain of blocks, while the state database contains the current values of key-value pairs, which have been modified and created by clients [21]. Each HLF channel has its own channel-specific ledger, and peers can participate in multiple HLF channels. Thus, a peer holds and maintains each copied ledger of the HLF channels, in which it exists as a member.

4) *Organization*: The organization refers to a group, which peers appertain to. An organization is joined to a HLF network by the blockchain service provider. To this end, the organization adds the membership service provider, which is to provide credentials to clients and peers, to the HLF network. In other words, a peer is affiliated with at least one organization to serve as a valid node in the HLF network.

5) *Chaincode*: The chaincode (i.e., smart contract) is a program, which defines several functions and business logics to modify retained data stored in the form of key-value pairs as well as to manage the ledger. In general, chaincodes are isolated for data integrity to protect themselves against unauthorized changes. An endorsing peer can invoke the chaincode to simulate the business logic that a client specified in a transaction proposal.

6) *Block Size*: The block size is one of the configurable parameters of the ordering service. This parameter defines the maximum number of transactions in one block, when endorsed transactions sent by clients stack up in the queue in the ordering service. A new block including the transactions is promptly exported from the ordering service the moment that the number of transactions in the queue reaches the pre-defined block size value.

7) *Block-generation Timeout*: The block-generation timeout is also one of the configurable parameters of the ordering service. This parameter defines the maximum time to wait for other transactions to generate a new block. When a first transaction arrives at the empty queue in the ordering service, a timer is identically set to the pre-defined block-generation timeout value. Once the timer expires, the ordering service generates a new block with all of the waiting transactions, even if the block affords to possess more transactions. This parameter prevents transactions from consuming too much time in the queue, in case that the number of new transactions delivered to the ordering service is insufficient to reach the configured block size value.

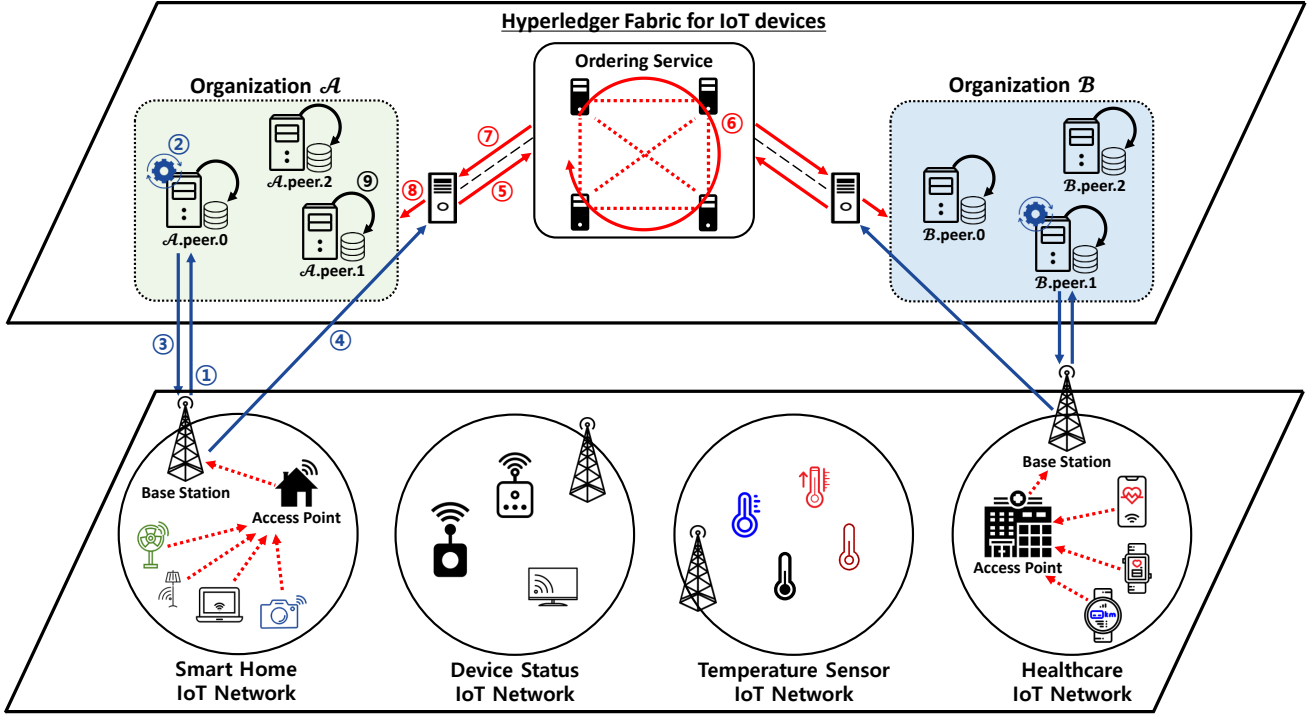


Fig. 1: The structure of HLF-based IoT networks

B. Transaction Flow

Transactions in HLF are processed through three phases to be appended: endorsing phase, ordering phase, and validation phase. Each phase has characteristic operations and objectives, which are essential not only to keep blockchain systems tamper-proof, but also to ensure data integrity. In other words, the transaction flow is an important part to sustain a HLF blockchain network. In this subsection, we describe the transaction-processing stages and provide detailed explanations of the three-phased flow.

1) *Endorsing Phase*: The endorsing phase is the first phase that a transaction proposal from the client enters. The main objective of this phase is to receive endorsements as proposal simulation results for the next step. In order to successfully pass this phase, the client needs to ask the sufficient number of endorsing peers to simulate the transaction proposal, according to the endorsement policy. Note that the endorsement policy specifies by which endorsing peers transaction proposals have to be endorsed [22]. If a transaction goes to the next phase without sufficient endorsements, it is marked as invalid in the validation phase.

When the endorsing peers receive the proposal, they each simulate the request against their local status using the specified chaincode. In consequence, they respond to the client with endorsements, containing a read/write set. The read set includes the key to update and its latest version, which already has been committed to ledger previously, while the write set includes the key to update and its new value, with which the client hopes to update the value of the key. Note that this phase does not lead to a ledger update. The client, then, investigates that whether the delivered endorsements have

exactly the same simulation results (i.e., the new value of the key) from one another. If they are identical, the endorsements are collected in the form of a transaction, and transmitted to the ordering service for the ordering phase. On the other hands, if they have different simulation results, the client discards the endorsements and refuses to continue processing the transaction proposal.

2) *Ordering Phase*: The ordering phase is the second phase, in which every delivered transaction is ordered chronologically per HLF channel in the ordering service. The main objective of this phase is to collect transactions and to produce new blocks. The ordering service amasses all transactions from every registered HLF channel separately for data confidentiality, then generates a new block for each HLF channel. The new block is transmitted to the corresponding channel for the validation phase. The ordering service is a cluster composed of several nodes, which are eligible for performing the predefined consensus protocol. In this paper, we focus on the Kafka/ZooKeeper-based ordering service, which is currently the most widely used implementation method.

3) *Validation Phase*: The validation phase is the last phase, in which the new block is validated by each peer individually. A peer that has received the block conducts two verifications on it sequentially in this phase: (1) Validation system chaincode (VSCC) verification and (2) Multi-version concurrency control (MVCC) verification. The VSCC verification is to make sure that a transaction has been endorsed by proper endorsing peers. If a transaction does not hold appropriate endorsements, it is prohibited from updating the ledger. Therefore, on the basis of the endorsement policy defining by which endorsing peers transactions have to be endorsed for

commitment, every transaction in the block is successively investigated and marked as either valid or invalid in this verification stage.

The MVCC verification is to investigate if the key versions captured during the endorsing phase still remain the same as those in the current ledger locally owned by the peer [20]. If they are the same as each other, the transaction is allowed to update the ledger with the data, and the key version is changed. In contrast, the transaction is considered as invalid if any of the previously conveyed transactions has successfully updated the identical data (i.e., the same key-value) ahead of it, because a key-version of data change happens each time the data is successfully updated [22].

C. HLF-based IoT Networks

Figure 1 demonstrates HLF-based IoT networks equipped with a HLF network preserving data generated from IoT devices. A group of IoT devices can establish a specific IoT network, while HLF facilitates IoT networks to exploit the blockchain storage for data management. As can be seen in Fig. 1, IoT devices in the smart home and healthcare IoT networks are currently activated to transmit their data to each access point (AP) that they are connected to.

In the smart home IoT network, for example, the smart appliances transmit data, which is necessary to be stored to the blockchain system, then AP conveys the delivered data to the nearest base station (BS), then the BS entitled to access the HLF network starts to communicate with the corresponding endorsing peer (i.e., $\mathcal{A}.peer.0$) in order to append the data to the ledger as a client. Note that IoT devices are considered to be incapable of joining the HLF network or working as a client by themselves because they may not have efficient resources to proceed with the authentication processes and to maintain certificates. The proposal sent from the BS is received by the endorsing peer, and the endorsing peer simulates the data against its own ledger, using the smart contract. Upon completion of the transaction simulation process, the endorsing peer returns the result to the BS. Note that if the endorsement policy appoints multiple peers to endorsing peers, the BS is required to ensure that all returned results are identical to one another. After the BS delivers the simulation result (i.e., endorsement) to the ordering service in the form of a transaction, the ordering service amasses endorsed transactions and creates a new block per HLF channel. Note that the ordering service can assort collected transactions, depending on their sources for privacy by constructing additional HLF channels. The new block including the transaction is conveyed to the peers belonging to the corresponding channel for the validation phase, then the block is finally committed to the ledger if it is successfully marked as valid.

D. Latency Types in HLF

In Section III.C, we instantiate HLF-based IoT networks, where data from the smart home IoT network is committed to the ledger in order. Before modeling the HLF latency, we first divide the total elapsed time of the data in the HLF network according to the transaction-processing stages, then

provide the technical definition of each latency type, namely, endorsing latency, ordering latency, validation latency, and ledger-commitment (i.e., total latency). Note that we exclude the communication latency from IoT devices to a BS not for specific cases, but for a wide range of applicable use cases.

- The endorsing latency refers to the time taken to ask endorsing peers to endorse a transaction and to receive their responses. To be specific, it is defined in this paper as the sum of latency 1, 2, 3, and 4 in Fig. 1.
- The ordering latency refers to the time taken to receive the transaction and to await until exported as a new block. It is defined in this paper as the sum of latency 5, 6, 7, and 8 in Fig. 1. Note that latency 6 consists of the consensus time and the waiting time for other transactions to be released as part of a new block from each transaction's level. On the other hand, the latency 8 is the transmission time and waiting time of the new block for the validation phase. Therefore, it may be considered as part of the validation latency, but is included in the histograms in Figs. 2 and 3. Note that the latency 8 may be highly likely to work as a performance bottleneck if the previous block requires much time to be validated.
- The validation latency refers to the time taken to validate and commit the new block. Transactions in the same block are sequentially validated, but committed all together as a batch. Therefore, technically speaking, they all have the identical validation latency from one another. Note that the validation latency is not measured at a committing peer, but is at an endorsing peer in this paper. To be specific, this latency is defined in this paper as latency 9 at an endorsing peer in Fig. 1.
- The ledger-commitment latency (i.e., total latency) refers to the time taken to completely process a transaction from the beginning. It is defined in this paper as the sum of the three latency types explained above.

IV. HLF LATENCY MODELING

Using probability distribution fitting techniques, we fit a curve to each latency histogram of the endorsing latency, ordering latency, validation latency, and ledger-commitment latency. We then find it possible to define their histograms as existing probability distributions. The probability density functions (PDFs) and cumulative distribution functions (CDFs) of three probability distributions, which are determined as best-fit distributions through our experiments, are first introduced. Note that the best-fit distribution refers to the probability distribution resulting in the smallest difference from a captured data set produced from repeated observations out of candidates. Subsequently, we not only provide a ledger-commitment latency model along with goodness-of-fit test results, but also reveal some cases, in which the best-fit distribution for the ledger-commitment latency does not work.

Even though it is claimed that throughput is more important than latency in [16], the significance of latency does not need to be devalued because latency and throughput can not only correlate with each other, but also influence comprehensive performance. For example, in age of information (AoI), which

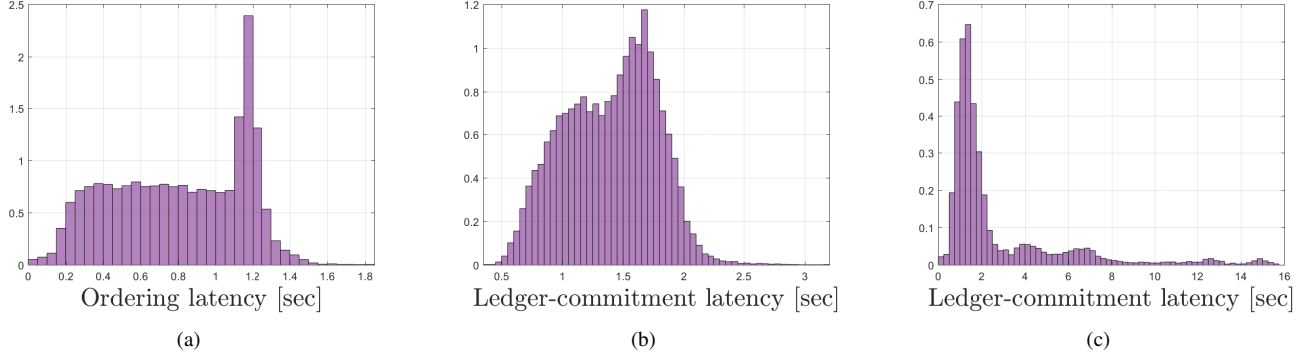


Fig. 2: Ordering latency and ledger-commitment latency histograms from some scenarios, where the probability distribution fitting method based on gamma distributions is not effective.

has been recently proposed to quantify and estimate data freshness, both latency and throughput play a key role. Besides, in terms of reliability, even if two different parameter setups result in the identical throughput from each other, it is difficult to believe that they are all reliable because either of them may have large variance among each transaction's latency [23]. Thus, the significances of latency and throughput are equivalent.

A. Experimental Setup

For the implementation of our HLF network, we exploit the HLF v1.3 sample network provided at [21] on one physical machine. The physical machine is with Intel(R) Xeon W-2155 @ 3.30 GHz and 16 GB RAM. Consequently, we newly bring up a Kafka/ZooKeeper-based ordering service consisting of four kafka nodes (i.e. ordering nodes) and three frontend nodes that are connected to the Kafka cluster in the network. Note that the frontend node is not only to inject transactions from clients into the Kafka cluster, but also to receive new blocks and to distribute them via the gossip protocol. The number of endorsing peers and committing peers in the HLF network are one and two, respectively. Note that the number of committing peers may not be able to affect the histogram shape because they are not allowed to involve themselves in the transaction-processing steps, but to validate new blocks and retain copied ledgers only.

Each test run includes 1,000 transaction proposals to submit, and all transactions to update each stored key-value set are conveyed to the endorsing peer in the HLF network one after another, possessing appropriate arguments for the *changeCarOwner* function defined in the *Fabcar* chaincode at [21]. Each of the frontend nodes has an equal probability of being selected to receive a transaction and to distribute a new block. Note that every generated transaction updates a different key-value from each other only once, therefore, the impact of MVCC violation is not considered in this paper. All transactions are generated at a certain rate per second, denoted as λ_{txn} . In this experiments, we not only vary this transaction generation rate λ_{txn} , but also measure the endorsing latency, ordering latency, validation latency, and ledger-commitment latency in order to analyze the impact of

increasing λ_{txn} . Note that the inter-generation times among all generated transactions follow an exponential distribution.

B. Best-fit Probability Distributions

The HLF network, as described in Section III-D, includes all the latency types (i.e., endorsing latency, ordering latency, validation latency, and ledger-commitment latency). In order to provide a latency model by fitting curves to the histograms, we first capture at least over 20,000 transaction samples for latency histograms, then seek out a best-fit probability distribution for each latency histogram. The discovered best-fit distributions are introduced with their PDFs and CDFs as in the following.

1) *Exponential Distribution*: The exponential distribution is the probability distribution of time intervals in a Poisson process. This distribution has the PDF as:

$$f(x) = \lambda e^{-\lambda x} \quad (1)$$

The CDF of the exponential distribution is given as follows:

$$F(x) = 1 - e^{-\lambda x} \quad (2)$$

Note that λ is the rate parameter for $\lambda > 0$. In this paper, the exponential distribution is used for probability distribution fitting to the endorsing latency.

2) *Gamma Distribution*: The gamma distribution is a two parameter frequency distribution [24]. The PDF of the gamma distribution is defined for $\alpha > 0$, $\beta > 0$ as:

$$f(x) = \frac{\beta^\alpha}{\Gamma(\alpha)} x^{\alpha-1} e^{-\beta x} \quad (3)$$

On the other hand, the CDF is given for $\alpha > 0$, $\beta > 0$ as below:

$$F(x) = \frac{1}{\Gamma(\alpha)} \gamma(\alpha, \beta x) \quad (4)$$

The gamma function, denoted as $\Gamma(\alpha)$, is defined for $\alpha > 0$ as follows:

$$\Gamma(\alpha) = \int_0^\infty x^{\alpha-1} e^{-x} dx \quad (5)$$

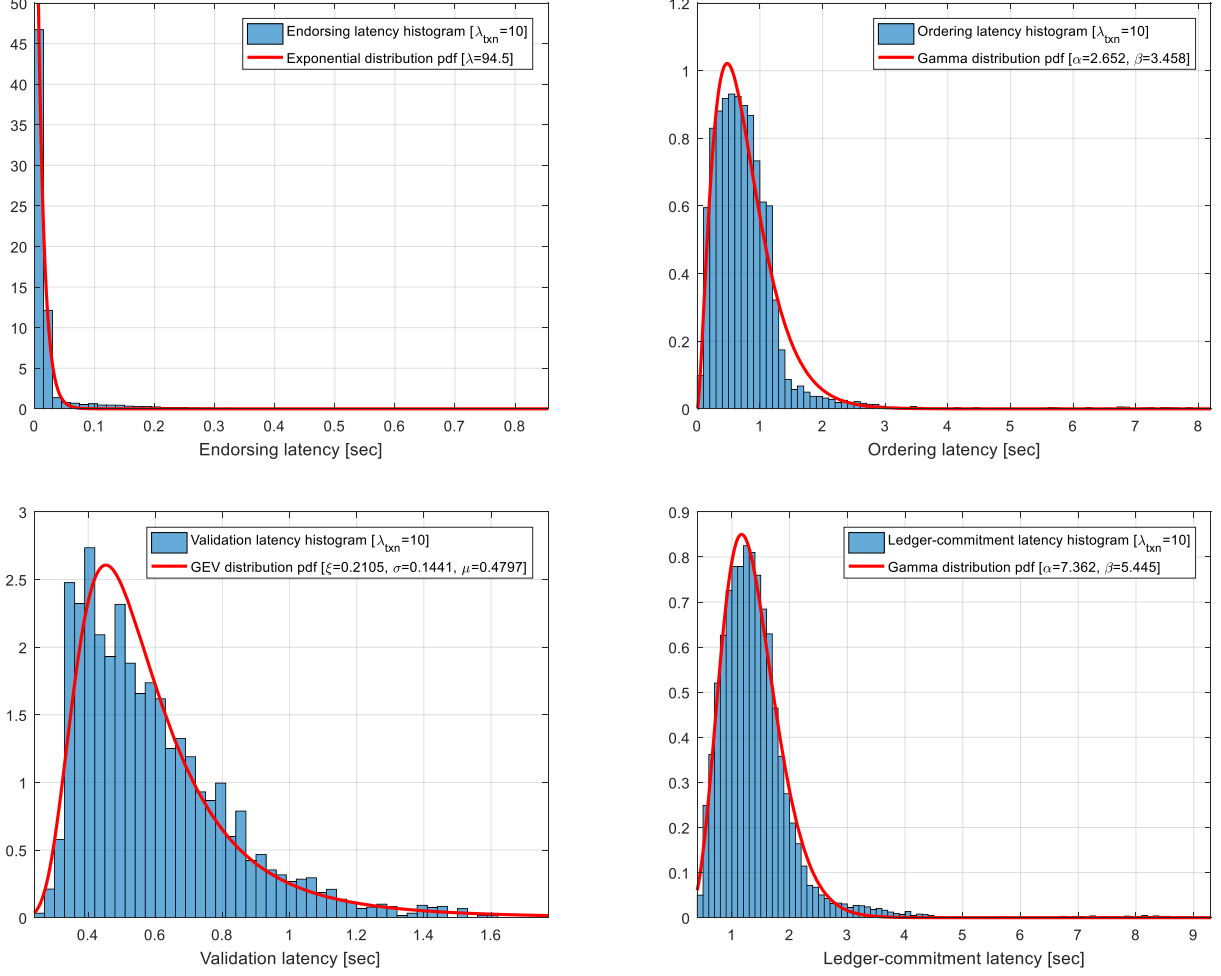


Fig. 3: The histograms of endorsing latency, ordering latency, validation latency, and ledger-commitment latency, where the block size is 10, block-generation timeout is 1 second, and transaction generation rate is 10 transactions/second.

The lower incomplete gamma function, denoted as $\gamma(\alpha, x)$, is defined for $\alpha > 0$, $x \geq 0$ as follows [25]:

$$\gamma(\alpha, x) = \int_0^x t^{\alpha-1} e^{-t} dt \quad (6)$$

Note that α is the shape parameter, and β is the inverse scale parameter (i.e., rate parameter). In this paper, the gamma distribution is used for probability distribution fitting to the ordering latency and ledger-commitment latency.

3) *Generalized Extreme Value (GEV) distribution*: The GEV distribution encompasses the three standard extreme value distributions: Gumbel ($\xi = 0$), Fréchet ($\xi > 0$), and Weibull ($\xi < 0$) [26]. Depending on the shape parameter, denoted as ξ , the GEV distribution results in one of the three probability distributions, which are also respectively referred to as GEV distribution's Type I, II, and III in the listed order above. The PDF of the GEV distribution is given as the following expression for $-\infty < x \leq \mu - \frac{\sigma}{\xi}$ when $\xi < 0$, for $\mu - \frac{\sigma}{\xi} \leq x < \infty$ when $\xi > 0$, and for $-\infty \leq x \leq \infty$ when $\xi = 0$ [27]:

$$f(x) = \begin{cases} \frac{\{1 + \xi (\frac{x-\mu}{\sigma})\}^{-[(\frac{1}{\xi})-1]}}{\sigma \exp\left\{\left(1 + \xi (\frac{x-\mu}{\sigma})\right)^{-\frac{1}{\xi}}\right\}}, & \text{if } \xi \neq 0 \\ \frac{1}{\sigma} \exp\left\{-\frac{x-\mu}{\sigma} - \exp\left[-\frac{x-\mu}{\sigma}\right]\right\}, & \text{if } \xi = 0 \end{cases} \quad (7)$$

On the other hand, the CDF of the GEV distribution is defined for $-\infty < x \leq \mu - \frac{\sigma}{\xi}$ when $\xi < 0$, for $\mu - \frac{\sigma}{\xi} \leq x < \infty$ when $\xi > 0$, and for $-\infty \leq x \leq \infty$ when $\xi = 0$ as follows:

$$F(x) = \begin{cases} \exp\left\{-\left(1 + \xi (\frac{x-\mu}{\sigma})\right)^{-\frac{1}{\xi}}\right\}, & \text{if } \xi \neq 0 \\ \exp\left\{-\exp\left\{-\frac{x-\mu}{\sigma}\right\}\right\}, & \text{if } \xi = 0 \end{cases} \quad (8)$$

Note that μ is the location parameter, and σ is the scale parameter. In this paper, the GEV distribution is used for probability distribution fitting to the validation latency. In our

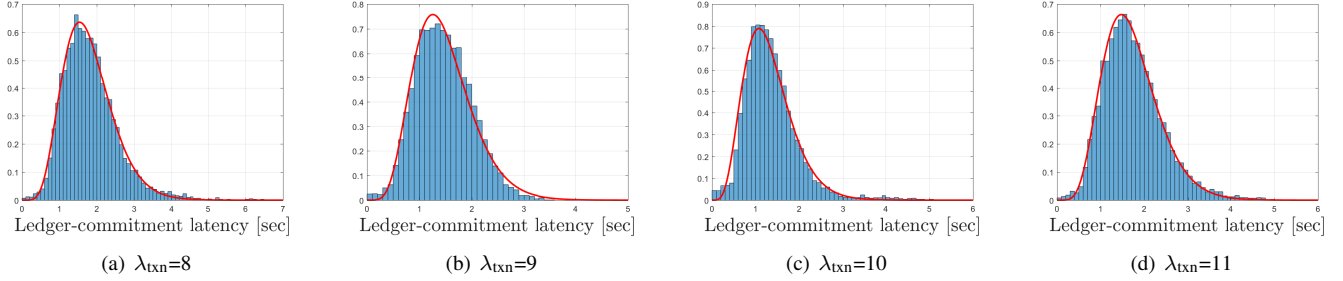


Fig. 4: Ledger-commitment latency model and gamma distributions with varying transaction generation rates, where the block size is 10 and block-generation timeout is 2 seconds.

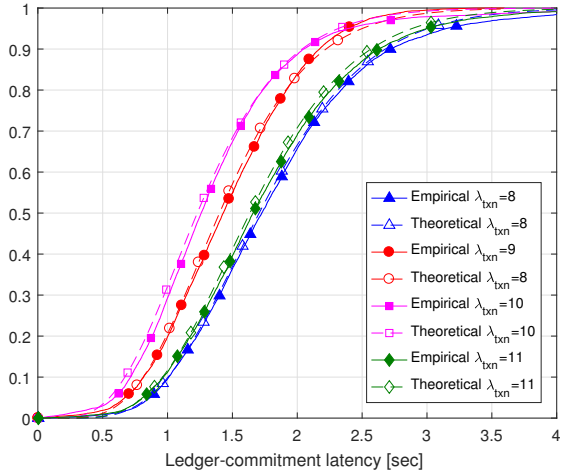


Fig. 5: Empirical CDFs and theoretical CDFs of Fig. 4.

observation, validation latency histograms have GEV distribution's Type II (i.e., the Fréchet distribution for $\xi > 0$) only.

C. Modeling Feasible Conditions

During the modeling process, it is found out that there exist some cases whose histograms of the ledger-commitment latency do not fit into a gamma distribution. In other words, probability distribution fitting based on gamma distributions is not always effective at configurable HLF parameter setups. We have discovered that two environments, in which a gamma distribution is an inappropriate description of their ledger-commitment latency shapes. Figures 2(b) and 2(c) demonstrate two ledger-commitment latency histograms measured in such different setups from each other, which are not well-matched with a gamma distribution.

As the first example, Figs. 2(a) and 2(b) illustrate ordering latency and ledger-commitment latency histograms, where the block size is 10, block-generation timeout is 1 second, and λ_{txn} is 3 transactions/second, respectively. If the timer in the ordering service expires before the waiting queue for new transactions becomes full, the collected transactions are immediately made into a new block, no matter how many transactions the new block possesses. This implies that

when most of generated blocks are influenced by the block-generation timeout parameter, the ordering latency of every first transaction inside each block is almost identical to the pre-defined block-generation timeout value. At this point, if the average number of transactions in one block is too small in comparison with the pre-defined block size value, the transactions whose observed ordering latency values are almost identical to the pre-defined block-generation timeout value are presented in the histogram with high frequency, and make a gamma distribution ineffective at fitting curves. In fact, the percentage of blocks influenced by the block-generation timeout is 99.803 in Figs. 2(a) and 2(b). This leaves a sharp increase around 1.2 seconds in Fig. 2(a) and two peaks around 1.2 and 1.6 seconds in Fig. 2(b).

On the other hand, if the block-generation rate of the ordering service is too high that peers cannot handle flooding new blocks promptly, the blocks have high waiting time consumed for entering the validation phase. Figure 2(c) demonstrates the ledger-commitment latency histogram, where the block size is 15, block-generation timeout is 0.75 seconds, and λ_{txn} is 10 transactions/second. In this case, most of the generated blocks are influenced by the block size parameter because λ_{txn} is high enough that new transactions are put into many generated blocks to the limit. As can be seen in Fig. 2(c), however, a gamma distribution is not a good match with the shape. Thus, this paper are not focused on these two cases.

D. Latency Modeling and Validation

In Section IV.A, we explain the experimental setup, from which the latency histograms are obtained, then discuss the probability distribution fitting feasible condition. We now illustrate the histograms of endorsing latency, ordering latency, validation latency, and ledger-commitment latency, then fit curves to them. In Fig. 3, when λ_{txn} is 10, the endorsing latency accords with the exponential distribution. The ordering latency and ledger-commitment latency match the gamma distributions. Especially, although the ordering latency leaves room for another best-fit probability distribution, the ledger-commitment latency is well-matched with the gamma distribution. On the other hand, the validation latency works with the GEV distribution.

Figure 4 demonstrates histograms of the ledger-commitment latency with each of their best-fit gamma distributions in the

TABLE I: Estimated gamma distribution parameters for the theoretical ledger-commitment latency and KS test results with varying the block-generation timeout, block size, and transaction generation rate values.

Timeout = 1[sec]		λ_{txn} [transactions/sec]				Timeout = 1[sec]		λ_{txn} [transactions/sec]			
Block size = 20		10	11	12	13	Block size = 25		17	18	19	20
Estimated $(\alpha_{\text{txn}}, \beta_{\text{txn}})$	(8.9573, 5.5858)	(9.5112, 6.0407)	(9.3159, 6.2078)	(10.0333, 6.2937)	Estimated $(\alpha_{\text{txn}}, \beta_{\text{txn}})$	(9.7902, 6.0267)	(9.1368, 6.131)	(9.005, 5.9462)	(8.2069, 5.395)		
Average KS statistic	0.0457	0.0466	0.0503	0.049	Average KS statistic	0.0504	0.0595	0.0564	0.051		
Empirical latency [sec]	1.6066	1.5767	1.4969	1.5891	Empirical latency [sec]	1.6141	1.4908	1.5098	1.5232		
Theoretical latency [sec]	1.6035	1.5745	1.5006	1.5941	Theoretical latency [sec]	1.6244	1.4902	1.5144	1.5212		

Timeout = 2[sec]		λ_{txn} [transactions/sec]				Timeout = 2[sec]		λ_{txn} [transactions/sec]			
Block size = 10		8	9	10	11	Block size = 20		15	16	17	18
Estimated $(\alpha_{\text{txn}}, \beta_{\text{txn}})$	(7.181, 4.0151)	(6.8603, 4.6625)	(5.6829, 4.355)	(7.1636, 4.1801)	Estimated $(\alpha_{\text{txn}}, \beta_{\text{txn}})$	(7.6898, 4.6474)	(8.4486, 5.1794)	(8.0874, 5.2866)	(8.3269, 4.8638)		
Average KS statistic	0.0388	0.0437	0.0457	0.0444	Average KS statistic	0.0358	0.0474	0.0419	0.0404		
Empirical latency [sec]	1.8289	1.4658	1.3517	1.7513	Empirical latency [sec]	1.6587	1.6406	1.5323	1.7437		
Theoretical latency [sec]	1.7884	1.4713	1.3049	1.7137	Theoretical latency [sec]	1.6566	1.6311	1.5297	1.712		

Timeout = 3[sec]		λ_{txn} [transactions/sec]				Timeout = 3[sec]		λ_{txn} [transactions/sec]			
Block size = 20		15	16	17	18	Block size = 30		23	24	25	26
Estimated $(\alpha_{\text{txn}}, \beta_{\text{txn}})$	(7.9739, 4.9723)	(7.608, 4.9499)	(7.0015, 4.9697)	(5.7078, 4.1482)	Estimated $(\alpha_{\text{txn}}, \beta_{\text{txn}})$	(8.0788, 4.6915)	(7.0546, 4.527)	(6.3698, 4.4257)	(7.3836, 4.8698)		
Average KS statistic	0.0382	0.0394	0.0403	0.0513	Average KS statistic	0.0369	0.0395	0.0468	0.0435		
Empirical latency [sec]	1.616	1.5351	1.3992	1.3902	Empirical latency [sec]	1.727	1.5652	1.4345	1.5125		
Theoretical latency [sec]	1.6036	1.537	1.4088	1.3759	Theoretical latency [sec]	1.722	1.5583	1.4392	1.5162		

λ_{txn} range from 8 to 11, and Fig. 5 shows empirical and theoretical CDFs. Table I shows estimated gamma distribution parameter pairs and goodness-of-fit test results obtained from a variety of HLF environments, including the estimated gamma distribution parameters of Fig. 4. We consider all captured data during one test run as outliers when their mean ledger-commitment latency value is remarkably longer than those of the other test runs. We exclude such outliers in a different way from [14]. Note that the median empirical results are compared to the estimated ones in [14]. In Fig. 4 and the corresponding results table (i.e., the third sub-table in Table I), the mean ledger-commitment latency decreases as λ_{txn} increases, allowing the ordering service to generate new blocks faster. However, the trend goes in the opposite direction when λ_{txn} becomes 11. This is because some new blocks gradually start to wait for the validation phase, due to the fast block-generation rate. Note that we leverage nonlinear regression to discover the best-fit parameters.

In order to validate and improve the reliability of our latency model, we demonstrate Kolmogorov-Smirnov (KS) test results for evaluating goodness-of-fit in Table I. Note that the estimated parameters and KS statistics are averaged over ten test runs at the 0.01 significance level. The critical value is then set to 0.0513, in other words, the latency model can be considered as reliable when the KS statistics value is smaller than 0.0513. Thus, the test passes with success for most of the cases in Table I, furthermore, the theoretical latency is still analogous to the empirical latency even in the cases that the test does not successfully pass.

Furthermore, when the average throughput is defined as the average number of completed transactions per second, the average throughput of HLF can also be estimated. In this

paper, the average ledger-commitment latency is defined as follows:

$$\mathbb{E}[T_{\text{total}}] = \frac{\sum_{i=1}^N t_i}{N} \quad (9)$$

where T_{total} is the total latency (i.e., ledger-commitment latency) when the block size and block-generation timeout are given, N is the total number of transmitted transactions, and t_i is the ledger-commitment latency of the i -th transaction.

On the other hand, the average throughput is defined as follows:

$$\frac{1}{\mathbb{E}[T_{\text{total}}]} = \frac{N}{\sum_{i=1}^N t_i} \quad (10)$$

Therefore, the average throughput can be obtained based on the definition of the average ledger-commitment latency.

V. INFLUENTIAL PARAMETER ANALYSIS ON LATENCY

From the viewpoint of an IoT device, which handles time-sensitive jobs and desires faster transaction commitment, the optimal design of HLF can be achieved by minimizing the ledger-commitment latency. As defined in Section III.A, the block size and block-generation timeout parameters are the important parameters to control producing new blocks in the ordering service. This implies that the block-generation rate of the ordering service, which is highly influential on the ledger-commitment latency and determined by the other parameters indirectly, also can be under control to minimize the ledger-commitment latency. Focusing on the two parameters, therefore, we first explore their impacts on the ledger-commitment latency in order to provide some insights on the methods

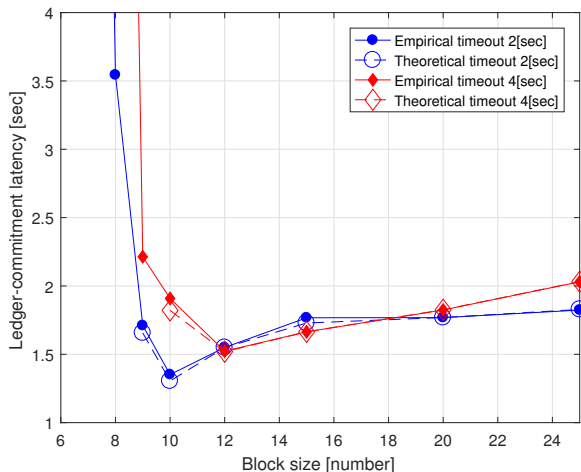


Fig. 6: Effect of block size on the ledger-commitment latency, where λ_{txn} is 10 and the block-generation timeout is 2 and 4 seconds.

for reducing and minimizing the ledger-commitment latency. Moreover, we reveal that 1) the optimal block size and block-generation timeout parameter values for the lowest latency exist, and 2) an increase in the block-generation rate leads to two conflicting effects on the ledger-commitment latency.

A. Impact of Block Size

As defined in Section III.A, the block size parameter is to define the maximum number of transactions in a block. Figure 6 illustrates the impact of the block size on the empirical and theoretical ledger-commitment latency. Note that we estimate it in a probability distribution fitting feasible range on the basis of Section IV.C. Before the block size reaches each of the optimal values resulting in the lowest ledger-commitment latency (i.e., 10 and 12 when the block-generation timeout is 2 and 4 seconds, respectively), the ledger-commitment latency decreases as the block size increases. This is because the block-generation rate of the ordering service becomes higher as the block size is smaller, preventing transactions from staying for a long time in the ordering service waiting queue. Thus, new blocks are generated and distributed too fast that the peers cannot promptly handle them. The new blocks gradually stack up in each peer's queue for the validation with high queueing delays (i.e., each block's waiting time in the latency 8 in Fig. 1). However, as the block size increases, the ledger-commitment latency decreases and finally becomes lowest due to reduced block-generation rate. Note that the probability distribution fitting method does not work in this case as explained in Section IV.C.

When the block size is larger than the optimal value, on the other hand, the ledger-commitment latency increases, then saturates shortly. This is because transactions to be included into a block cannot help waiting longer for others as the block size increases, so the ordering latency increases. Nonetheless, the ledger-commitment latency does not increase infinitely despite of increase in the block size because the timer for the block-

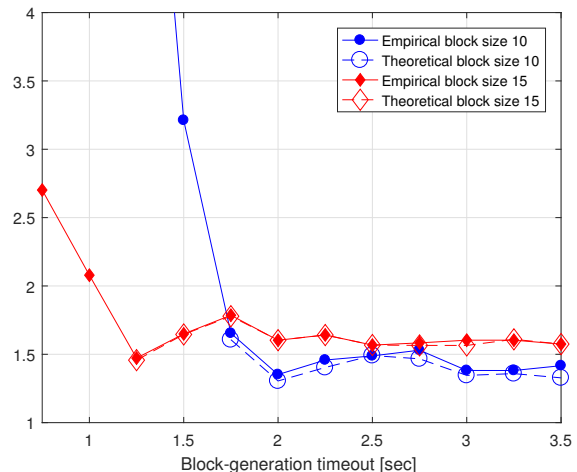


Fig. 7: Effect of block-generation timeout on the ledger-commitment latency, where λ_{txn} is 10 and the block size is 10 and 15.

generation timeout starts to expire, and waiting transactions are forced into forming a new block without awaiting others until the number of waiting transactions becomes identical to the block size from some point on. Hence, the ledger-commitment latency ends up saturating as the block-generation timeout is fixed in Fig. 6. Note that the case when the block-generation timeout is set to 4 seconds in Fig. 6 requires a much larger block size for saturation.

B. Impact of Block-generation Timeout

The block-generation timeout parameter is to prevent waiting transactions to be included into a block from spending long time in the ordering service for better performance. Figure 7 demonstrates the impact of the block-generation timeout on the empirical and theoretical ledger-commitment latency. The ledger-commitment latency decreases as the block-generation timeout increases until the block-generation timeout reaches each of the optimal values resulting in the lowest ledger-commitment latency (i.e., 2 and 1.25 seconds when the block size is 10 and 15, respectively). Besides, the ledger-commitment latency reversely increases with the block-generation timeout for the same reasons as explained in Section V.A.

However, different from Fig. 6, the ledger-commitment latency slightly decreases and ends up saturating as Fig. 6. We presume that this slight decrease is due to the ordering latency and validation latency. To be specific, when the block-generation timeout keeps increasing, the queueing delay to enter the validation phase decreases and finally touches zero. On the other hand, the rest of the ordering latency excluding the latency 8 in Fig. 1 and validation latency increase, although they saturate later. In this sense, when the ledger-commitment latency increases with the block-generation timeout, the ordering latency and validation latency still increase, while the queueing delay for the validation phase decreases steadily (i.e., from 2 to 2.75 seconds and from 1.25 to 1.75 seconds when the

block size is 10 and 15, respectively). However, the ordering latency and validation latency start to saturate because of the block size parameter ahead of the queuing delay, while the queuing delay for the validation phase decreases a bit longer, then disappears. Thus, it is concluded that each increase in the block size and block-generation timeout cannot affect the ledger-commitment latency infinitely, but makes it saturate when the other parameters are fixed.

VI. CONCLUSIONS

In this paper, we propose a latency model of HLF v1.3, which is instantiated as HLF-based IoT networks, where each specific IoT network can deposit permanent data in the HLF blockchain network for data integrity and auditability. To this end, we first implement a HLF network on our physical machine and embed a Kafka/ZooKeeper ordering service into it. In an empirical approach, we construct histograms using captured transaction latency samples, then develop a hypothesis that the ledger-commitment latency is modeled with a gamma distribution in some configurable setup range. Introducing the KS test to evaluate goodness-of-fit, we prove that our latency model is reliable. In the sequel, considering the characteristic that IoT devices handle latency critical tasks in general, we analyze the impacts of two influential HLF parameters on the ledger-commitment latency, in order to provide practical insights on reducing and optimizing the ledger-commitment latency. We hope that this paper would serve as guidelines to theoretically estimating the ledger-commitment latency and to implementing HLF with the optimal design for HLF-based IoT networks.

REFERENCES

- [1] A. Dorri, S. S. Kanhere, R. Jurdak, and P. Gauravaram, "Blockchain for IoT security and privacy: The case study of a smart home," in *Proc. IEEE Int. Conf. Pervasive Comput. Commun. Workshops (PerCom WKSHPs)*, Kona, HI, USA, Mar. 2017, pp. 1–6.
- [2] T. T. A. Dinh, J. Wang, G. Chen, R. Liu, B. C. Ooi, and K.-L. Tan, "BLOCKBENCH: A framework for analyzing private blockchains," in *Proc. ACM Int. Conf. Manag. of data*, Chicago, IL, USA, May 2017, pp. 1–16.
- [3] T. T. A. Dinh, R. Liu, M. Zhang, G. Chen, B. C. Ooi, and J. Wang, "Untangling blockchain: A data processing view of blockchain systems," *IEEE Trans. Knowl. Data Eng.*, vol. 30, no. 7, pp. 1366–1385, Jul. 2018.
- [4] S. Pongnumkul, C. Siripanpornchana, and S. Thajchayapong, "Performance analysis of private blockchain platforms in varying workloads," in *Proc. Int. Conf. Comput. Commun. Netw. (ICCCN)*, Vancouver, BC, Canada, Aug. 2017, pp. 1–6.
- [5] P. Thakkar, S. Nathan, and B. Viswanathan, "Performance benchmarking and optimizing Hyperledger Fabric blockchain platform," in *Proc. IEEE Int. Symp. Model., Anal., Simul. Comput. Telecommun. Syst. (MAS-COTS)*, Milwaukee, WI, USA, Sep. 2018, pp. 1–13.
- [6] S. Shalaby, A. A. Abdellatif, A. Al-Ali, A. Mohamed, A. Erbad, and M. Guizani, "Performance evaluation of Hyperledger Fabric," in *Proc. IEEE Int. Conf. Inform., IoT, Enabling Technol. (ICIOT)*, Doha, Qatar, Feb. 2020, pp. 1–6.
- [7] M. Kuzlu, M. Pipattanasomporn, L. Gurses, and S. Rahman, "Performance analysis of a Hyperledger Fabric blockchain framework: Throughput, latency, and scalability," in *Proc. IEEE Int. Conf. Blockchain (Blockchain)*, Atlanta, GA, USA, Jul. 2020, pp. 1–5.
- [8] Q. Nasir, I. A. Qasse, M. A. Talib, and A. B. Nassif, "Performance analysis of Hyperledger Fabric platforms," *Secur. Commun. Netw.*, vol. 2018, no. 1, pp. 1–14, Sep. 2018.
- [9] H. Lee, C. Yoon, S. Bae, S. Lee, K. Lee, S. Kang, K. Sung, and S. Min, "Multi-batch scheduling for improving performance of Hyperledger Fabric based IoT applications," in *Proc. IEEE Global Commun. Conf. (GLOBECOM)*, Waikoloa, HI, USA, Dec. 2019, pp. 1–6.
- [10] T. S. L. Nguyen, G. Jourjon, M. Potop-Butucaru, and K. L. Thai, "Impact of network delays on Hyperledger Fabric," in *Proc. IEEE Int. Conf. Comput. Commun. Workshops (INFOCOM WKSHPs)*, Paris, France, Apr. 2019, pp. 1–6.
- [11] L. Foschini, A. Gavagna, G. Martuscelli, and R. Montanari, "Hyperledger Fabric blockchain: Chaincode performance analysis," in *Proc. IEEE Int. Conf. Commun. (ICC)*, Dublin, Ireland, Jun. 2020, pp. 1–6.
- [12] S. Wang, "Performance evaluation of Hyperledger Fabric with malicious behavior," in *Proc. Int. Conf. Blockchain (ICBC)*, San Diego, CA, USA, Jun. 2019, pp. 1–9.
- [13] T. Nakaïke, Q. Zhang, Y. Ueda, T. Inagaki, and M. Ohara, "Hyperledger Fabric performance characterization and optimization using GoLevelDB benchmark," in *Proc. IEEE Int. Conf. Blockchain Cryptocurrency (ICBC)*, Toronto, ON, Canada, May 2020, pp. 1–9.
- [14] H. Sukhwani, J. M. Martinez, X. Chang, K. S. Trivedi, and A. Rindos, "Performance modeling of PBFT consensus process for permissioned blockchain network (Hyperledger Fabric)," in *Proc. Symp. Rel. Distrib. Syst. (SRDS)*, Hong Kong, China, Sep. 2017, pp. 1–3.
- [15] H. Sukhwani, N. Wang, K. S. Trivedi, and A. Rindos, "Performance modeling of Hyperledger Fabric (permissioned blockchain network)," in *Proc. IEEE Int. Symp. Netw. Comput. Appl. (NCA)*, Cambridge, MA, USA, Nov. 2018, pp. 1–10.
- [16] P. Yuan, K. Zheng, X. Xiong, K. Zhang, and L. Lei, "Performance modeling and analysis of a Hyperledger-based system using GSPN," *Comput. Commun.*, vol. 153, no. 1, pp. 117–124, Mar. 2020.
- [17] L. Jiang, X. Chang, Y. Liu, J. Mistic, and V. B. Mistic, "Performance analysis of Hyperledger Fabric platform: A hierarchical model approach," *Peer Peer Netw. Appl.*, vol. 13, no. 3, pp. 1014–1025, Jan. 2020.
- [18] J. Sousa, A. Bessani, and M. Vukolic, "A Byzantine fault-tolerant ordering service for the Hyperledger Fabric blockchain platform," in *Proc. IEEE/IFIP Int. Conf. Dependable Syst. Netw. (DSN)*, Luxembourg City, Luxembourg, Jun. 2018, pp. 1–8.
- [19] <https://www.hyperledger.org>.
- [20] E. Androulaki, A. Barger, V. Bortnikov, and C. Cachin, "Hyperledger Fabric: A distributed operating system for permissioned blockchains," in *Proc. Eur. Conf. Comput. Syst. (EuroSys)*, Porto, Portugal, Jan. 2018, pp. 1–15.
- [21] <https://hyperledger-fabric.readthedocs.io/en/release-1.3>.
- [22] S. Lee, M. Kim, R.-H. Hsu, and T. Q. S. Quek, "Is blockchain suitable for data freshness? – Age-of-Information perspective," *arXiv preprint arXiv:2006.02735*, to appear in *IEEE Netw.*, pp. 1–7, Jun. 2020.
- [23] A. Bruton, J. H. Conway, and S. T. Holgate, "Reliability: What is it, and how is it measured?" *Physiotherapy*, vol. 86, no. 2, pp. 94–99, Feb. 2000.
- [24] H. S. C. Thom, "A note on the gamma distribution," *Mon. Weather Rev.*, vol. 86, no. 4, pp. 117–122, Apr. 1958.
- [25] G. J. O. Jameson, "The incomplete gamma functions," *Math. Gaz.*, vol. 100, no. 548, pp. 298–306, Jul. 2016.
- [26] T. G. Bali, "The generalized extreme value distribution," *Econ. Lett.*, vol. 79, no. 3, pp. 423–427, Jan. 2003.
- [27] W. Huang, S. Xu, and S. Nnaji, "Evaluation of GEV model for frequency analysis of annual maximum water levels in the coast of United States," *Ocean Eng.*, vol. 35, no. 11, pp. 1132–1147, Aug. 2008.